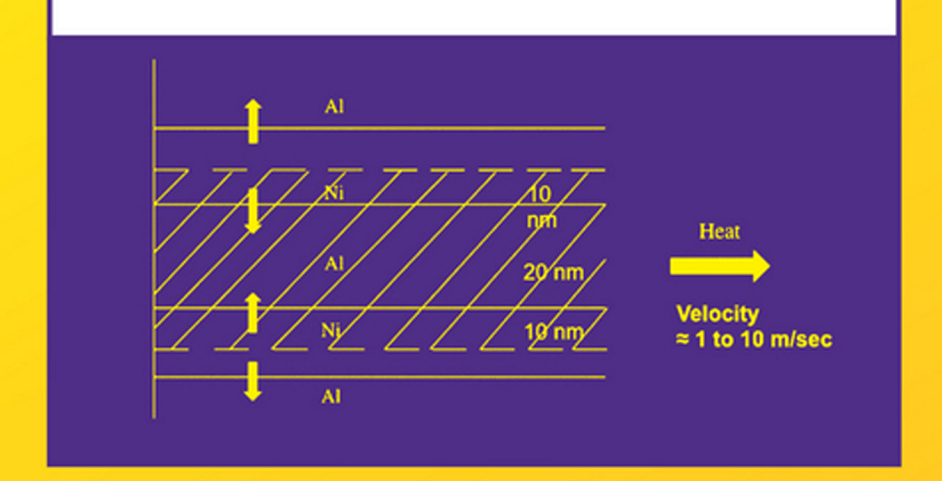
Kinetics in Nanoscale Materials



KING-NING TU ANDRIY M. GUSAK



KINETICS IN NANOSCALE MATERIALS

KINETICS IN NANOSCALE MATERIALS

KING-NING TU ANDRIY M. GUSAK



Cover Design: Wiley

Cover Image: Courtesy of the authors

Copyright © 2014 by John Wiley & Sons, Inc. All rights reserved.

Published by John Wiley & Sons, Inc., Hoboken, New Jersey. Published simultaneously in Canada.

No part of this publication may be reproduced, stored in a retrieval system, or transmitted in any form or by any means, electronic, mechanical, photocopying, recording, scanning, or otherwise, except as permitted under Section 107 or 108 of the 1976 United States Copyright Act, without either the prior written permission of the Publisher, or authorization through payment of the appropriate per-copy fee to the Copyright Clearance Center, Inc., 222 Rosewood Drive, Danvers, MA 01923, (978) 750-8400, fax (978) 750-4470, or on the web at www.copyright.com. Requests to the Publisher for permission should be addressed to the Permissions Department, John Wiley & Sons, Inc., 111 River Street, Hoboken, NJ 07030, (201) 748-6011, fax (201) 748-6008, or online at http://www.wiley.com/go/permission.

Limit of Liability/Disclaimer of Warranty: While the publisher and author have used their best efforts in preparing this book, they make no representations or warranties with respect to the accuracy or completeness of the contents of this book and specifically disclaim any implied warranties of merchantability or fitness for a particular purpose. No warranty may be created or extended by sales representatives or written sales materials. The advice and strategies contained herein may not be suitable for your situation. You should consult with a professional where appropriate. Neither the publisher nor author shall be liable for any loss of profit or any other commercial damages, including but not limited to special, incidental, consequential, or other damages.

For general information on our other products and services or for technical support, please contact our Customer Care Department within the United States at (800) 762-2974, outside the United States at (317) 572-3993 or fax (317) 572-4002.

Wiley also publishes its books in a variety of electronic formats. Some content that appears in print may not be available in electronic formats. For more information about Wiley products, visit our web site at www.wiley.com.

Library of Congress Cataloging-in-Publication Data:

Tu, K. N. (King-Ning), 1937-

Kinetics in nanoscale materials / by King-Ning Tu, Andriy Gusak.

pages cm

Summary: "As the ability to produce nanomaterials advances, it becomes more important to understand how the energy of the atoms in these materials is affected by their reduced dimensions. Written by an acclaimed author team, Kinetics in Nanoscale Materials is the first book to discuss simple but effective models of the systems and processes that have recently been discovered. The text, for researchers and graduate students, combines the novelty of nanoscale processes and systems with the transparency of mathematical models and generality of basic ideas relating to nanoscience and nanotechnology"—Provided by publisher.

"Published simultaneously in Canada"-Title page verso.

Includes bibliographical references and index.

ISBN 978-0-470-88140-8 (hardback)

- 1. Nanostructured materials. 2. Chemical kinetics. 3. Nanostructured materials-Analysis.
- 4. Nanostructured materials-Computer simulation. I. Gusak, Andriy M. II. Title.

TA418.9.N35T8 2014

620.1'1599-dc23

2013042096

Printed in the United States of America.

CONTENTS

PREF	FACE		ix
CHAP	TER 1 II	NTRODUCTION TO KINETICS IN NANOSCALE MATERIALS	1
1.1	Introduc	tion 1	
1.2	Nanosph	ere: Surface Energy is Equivalent to Gibbs—Thomson Potential 3	
1.3	Nanosph	ere: Lower Melting Point 6	
1.4	Nanosph	ere: Fewer Homogeneous Nucleation and its Effect on Phase Diagram	10
1.5	Nanosph	ere: Kirkendall Effect and Instability of Hollow Nanospheres 13	
1.6		ere: Inverse Kirkendall Effect in Hollow Nano Alloy Spheres 17	
1.7	_	ere: Combining Kirkendall Effect and Inverse Kirkendall Effect on	
		ric Bilayer Hollow Nanosphere 18	
1.8		ole: Instability of a Donut-Type Nano Hole in a Membrane 19	
1.9		e: Point Contact Reactions Between Metal and Silicon Nanowires 21	
1.10		e: Nanogap in Silicon Nanowires 22	
1.11		e: Lithiation in Silicon Nanowires 26	
1.12		re: Point Contact Reactions Between Metallic Nanowires 27	
1.13		in Film: Explosive Reaction in Periodic Multilayered Nano Thin Films	28
1.14		icrostructure in Bulk Samples: Nanotwins 30	
1.15		icrostructure on the Surface of a Bulk Sample: Surface Mechanical Attri	10n
		nt (SMAT) of Steel 32	
	Reference Problems		
	Problems	S 35	
CHAP	TER 2 L	INEAR AND NONLINEAR DIFFUSION	37
2.1	Introduc	tion 37	
2.2	Linear D		
	2.2.1	Atomic Flux 39	
	2.2.2	Fick's First Law of Diffusion 40	
	2.2.3	Chemical Potential 43	
	2.2.4	Fick's Second Law of Diffusion 45	
	2.2.5	Flux Divergence 47	
	2.2.6	Tracer Diffusion 49	
	2.2.7	Diffusivity 51	
	2.2.8	Experimental Measurement of the Parameters in Diffusivity 53	
2.3	Nonlinea	ar Diffusion 57	
	2.3.1		
	2.3.2	Nonlinear Effect due to Thermodynamic Consideration 59	
	2.3.3	Combining Thermodynamic and Kinetic Nonlinear Effects 62	
	Reference	ces 63	
	Problem	s 64	

СНАР	IER 3 KIRKENDALL EFFECT AND INVERSE KIRKENDALL EFFECT	67
3.1	Introduction 67	
3.2	Kirkendall Effect 69	
	3.2.1 Darken's Analysis of Kirkendall Shift and Marker Motion 72	
	3.2.2 Boltzmann and Matano Analysis of Interdiffusion Coefficient 76	
	3.2.3 Activity and Intrinsic Diffusivity 80	
	3.2.4 Kirkendall (Frenkel) Voiding Without Lattice Shift 84	
3.3	Inverse Kirkendall Effect 84	
0.0	3.3.1 Physical Meaning of Inverse Kirkendall Effect 86	
	3.3.2 Inverse Kirkendall Effect on the Instability of an Alloy Nanoshell 88	
	3.3.3 Inverse Kirkendall Effect on Segregation in a Regular Solution	
	Nanoshell 90	
3.4	Interaction Between Kirkendall Effect and Gibbs—Thomson Effect in the Formation	
3.4		Ш
	Problems 97	
CI I A D	DIDENING A MONG NA NODDECIDITATES	
CHAP	TER 4 RIPENING AMONG NANOPRECIPITATES	99
4.1	Introduction 99	
4.2	Ham's Model of Growth of a Spherical Precipitate (C_r is Constant) 101	
4.3	Mean-Field Consideration 103	
4.4	Gibbs-Thomson Potential 105	
4.5	Growth and Dissolution of a Spherical Nanoprecipitate in a Mean Field 106	
4.6	LSW Theory of Kinetics of Particle Ripening 108	
4.7	Continuity Equation in Size Space 113	
4.8	Size Distribution Function in Conservative Ripening 114	
4.9	Further Developments of LSW Theory 115 References 115	
	Problems 116	
CHAP ⁻	TER 5 SPINODAL DECOMPOSITION	118
5.1	Introduction 118	
5.2	Implication of Diffusion Equation in Homogenization and Decomposition 121	
5.3	Spinodal Decomposition 123	
	5.3.1 Concentration Gradient in an Inhomogeneous Solid Solution 123	
	5.3.2 Energy of Mixing to Form a Homogeneous Solid Solution 124	
	5.3.3 Energy of Mixing to Form an Inhomogeneous Solid Solution 126	
	5.3.4 Chemical Potential in Inhomogeneous Solution 129	
	5.3.5 Coherent Strain Energy 131	
	5.3.6 Solution of the Diffusion Equation 134	
	References 136	
	Problems 136	
CHAP	TER 6 NUCLEATION EVENTS IN BULK MATERIALS, THIN FILMS,	
	AND NANOWIRES	138
6.1	Introduction 138	

6.2 Thermodynamics and Kinetics of Nucleation

	6.2.1 Thermodynamics of Nucleation 140 6.2.2 Kinetics of Nucleation 143
6.3	Heterogeneous Nucleation in Grain Boundaries of Bulk Materials 148
	6.3.1 Morphology of Grain Boundary Precipitates 150
	6.3.2 Introducing an Epitaxial Interface to Heterogeneous Nucleation 151
	6.3.3 Replacive Mechanism of a Grain Boundary 154
6.4	No Homogeneous Nucleation in Epitaxial Growth of Si Thin Film on Si Wafer 156
6.5	Repeating Homogeneous Nucleation of Silicide in Nanowires of Si 160
	6.5.1 Point Contact Reactions in Nanowires 161
	6.5.2 Homogeneous Nucleation of Epitaxial Silicide in Nanowires of Si 164
	References 168
	Problems 168
CHAP	TER 7 CONTACT REACTIONS ON Si; PLANE, LINE, AND POINT
	CONTACT REACTIONS 17
7.1	Introduction 170
7.1	Bulk Cases 175
7.2	7.2.1 Kidson's Analysis of Diffusion-Controlled Planar Growth 175
	7.2.2 Steady State Approximation in Layered Growth of Multiple Phases 178
	7.2.3 Marker Analysis 179
	7.2.4 Interdiffusion Coefficient in Intermetallic Compound 182
	7.2.5 Wagner Diffusivity 186
7.3	Thin Film Cases 187
	7.3.1 Diffusion-Controlled and Interfacial-Reaction-Controlled Growth 187
	7.3.2 Kinetics of Interfacial-Reaction-Controlled Growth 188
	7.3.3 Kinetics of Competitive Growth of Two-Layered Phases 193
	7.3.4 First Phase in Silicide Formation 194
7.4	Nanowire Cases 196
	7.4.1 Point Contact Reactions 197
	7.4.2 Line Contact Reactions 202
	7.4.3 Planar Contact Reactions 208
	References 208
	Problems 209
CHAP	TER 8 GRAIN GROWTH IN MICRO AND NANOSCALE 21
8.1	Introduction 211
8.2	How to Generate a Polycrystalline Microstructure 213
8.3	Computer Simulation of Grain Growth 216
	8.3.1 Atomistic Simulation Based on Monte Carlo Method 216
	8.3.2 Phenomenological Simulations 217
8.4	Statistical Distribution Functions of Grain Size 219
8.5	Deterministic (Dynamic) Approach to Grain Growth 221
8.6	Coupling Between Grain Growth of a Central Grain and the Rest of Grains 225
8.7	Decoupling the Grain Growth of a Central Grain from the Rest of Grains in the
	Normalized Size Space 226
8.8	Grain Growth in 2D Case in the Normalized Size Space 229
8.9	Grain Rotation 231
	8.9.1 Grain Rotation in Anisotropic Thin Films Under Electromigration 232

viii CONTENTS

References 237 **Problems** 238 SELF-SUSTAINED REACTIONS IN NANOSCALE MULTILAYERED **CHAPTER 9** THIN FILMS 240 9.1 Introduction 240 9.2 The Selection of a Pair of Metallic Thin Films for SHS 9.3 A Simple Model of Single-Phase Growth in Self-Sustained Reaction 245 9.4 A Simple Estimate of Flame Velocity in Steady State Heat Transfer 250 9.5 Comparison in Phase Formation by Annealing and by Explosive Reaction in Al/Ni 9.6 Self-Explosive Silicidation Reactions 251 References 255 **Problems** 256 FORMATION AND TRANSFORMATIONS OF NANOTWINS **CHAPTER 10** IN COPPER 258 10.1 Introduction 258 10.2 Formation of Nanotwins in Cu 260 10.2.1 First Principle Calculation of Energy of Formation of Nanotwins 10.2.2 In Situ Measurement of Stress Evolution for Nanotwin Formation During Pulse Electrodeposition of Cu 264 10.2.3 Formation of Nanotwin Cu in Through-Silicon Vias 266 10.3 Formation and Transformation of Oriented Nanotwins in Cu 269 10.3.1 Formation of Oriented Nanotwins in Cu 10.3.2 Unidirectional Growth of Cu-Sn Intermetallic Compound on Oriented and Nanotwinned Cu 270 10.3.3 Transformation of (111) Oriented and Nanotwinned Cu to (100) Oriented Single Crystal of Cu 10.4 Potential Applications of Nanotwinned Cu 276 10.4.1 To Reduce Electromigration in Interconnect Technology 10.4.2 To Eliminate Kirkendall Voids in Microbump Packaging Technology 277 References 278 Problems 278 LAPLACE PRESSURE IN NONSPHERICAL NANOPARTICLE **APPENDIX A** 280 INTERDIFFUSION COEFFICIENT $\tilde{D} = C_R MG''$ APPENDIX B 282 APPENDIX C NONEQUILIBRIUM VACANCIES AND CROSS-EFFECTS ON INTERDIFFUSION IN A PSEUDO-TERNARY ALLOY 285 INTERACTION BETWEEN KIRKENDALL EFFECT AND APPENDIX D

INDEX 293

289

GIBBS-THOMSON EFFECT IN THE FORMATION OF A

SPHERICAL COMPOUND NANOSHELL

PREFACE

In the Department of Materials Science and Engineering at UCLA, three courses on kinetic processes in materials are being taught at the moment. The first course is MSE 131 on "Diffusion and Diffusion Related Phase Transformations," which is for upper undergraduate students. The textbook is "Phase Transformations in Metals and Alloys," 2nd edition, by D. A. Porter and K. E. Easterling, published by Chapman and Hall, London, 1992. The second course is MSE 223 on "Thin Film Materials Science," which is for first year graduate students. The textbooks are "Electronic Thin Film Science," by K. N. Tu, J. W. Mayer, and L. C. Feldman, published by Macmillan, New York, 1993, and "Electronic Thin Film Reliability," by K. N. Tu, published by Cambridge University Press, UK, 2011. The third course is MSE 201 on "Principle of Materials Science: Solid State Reactions," which is a mandatory course for Ph.D. students. It had been taught by Prof. Alan Ardell until his retirement in 2008. There is no textbook for this course, except the lecture notes by Prof. Ardell. One of the reasons that this book is written is to serve as the textbook for this course in the future. This book can also be used as a textbook for a kinetics course in the Department of Physics at Cherkasy National University, Cherkasy, Ukraine. Roughly speaking, MSE 131 covers mainly kinetics in bulk materials, MSE 223 emphasizes kinetics in thin films, and MSE 201 will focus on kinetics in nanoscale materials. It is worthwhile mentioning that kinetics in nanoscale materials is not completely new or very different from those in bulk and thin films. Actually, a strong link among them can be found, which is shown in this book. An example is the lower melting point of nanosize particles. In morphological instability of the solidification of bulk melt, the lower melting point of the tip of dendrite has been analyzed in detail.

Chapter 1 explains why the subject of kinetic processes in nanoscale materials is of interest. It begins with a discussion that the surface energy of a nanosphere is equal to its Gibbs—Thomson potential energy. This is implicit in the classical theory of homogeneous nucleation in bulk materials. Then, it is followed by several sections on some general kinetic behaviors of nanosphere, nanopore, nanowire, nanothin films, and nanomicrostructure in bulk materials. Specific topics on kinetics in nanoscale materials are covered by Chapter 2 on linear and nonlinear diffusion; Chapter 3 on Kirkendall effect and inverse Kirkendall effect; Chapter 4 on ripening among nanoprecipitates; Chapter 5 on spinodal decomposition; Chapter 6 on nucleation events in bulk materials, thin films, and nanowires; Chapter 7 on contact reactions on Si: plane, line, and point contact reactions; Chapter 8 on grain growth in micro and nanoscales; Chapter 9 on self-sustained explosive reactions in nanoscale multilayered thin films; and Chapter 10 on formation and transformation of nanotwins in Cu. In the last two chapters, applications of nanoscale kinetics are emphasized by the explosive reactions

X PRFFACE

for distance ignition or for local heating, and by nanotwinned Cu for interconnect and packaging technology for microelectronic devices.

In nanoscale materials, we encounter very high concentration gradient, very small curvature, very large nonequilibrium vacancies, very few dislocations, and yet very high density of grain boundaries and surfaces, and even nanotwins. They modify the driving force as well as the kinetic jump process. To model the nanoscale processes, our understanding of kinetic processes in bulk materials can serve as the stepping stone from where we enter into the nano region. On seeing the similarity between bulk and nanoscale materials, the readers can follow the link to obtain a better understanding of the kinetic processes in nanoscale materials. On seeing the difference, the readers will appreciate what modification is needed or what is new in the kinetic processes in nanoscale materials.

We would like to acknowledge that we have benefited greatly from the lecture notes by Prof. Alan Ardell on kinetics of homogeneous nucleation, spinodal decomposition, and ripening. We also would like to acknowledge that the second part of Chapter 2 on thermodynamic nonlinear effects on diffusion is taken from an unpublished 1986 IBM technical report written by Prof. Lydia Chiao in the Department of Physics at Georgetown University, Washington, DC. We apologize to the readers that because of our limited knowledge, we do not cover some of the very active and interesting topics of nanomaterials, such as the nucleation and growth of graphene on metal surfaces, VLS growth of nano Si wires, or interdiffusion in man-made superlattices. We hope that this book will help students and readers advance into these and other nanoscale kinetic topics in the future.

April 2014

King-Ning Tu and Andriy M. Gusak

INTRODUCTION TO KINETICS IN NANOSCALE MATERIALS

1.1	Introduction	I
1.2	Nanosphere: Surface Energy is Equivalent to Gibbs-Thomson Potential	3
1.3	Nanosphere: Lower Melting Point	6
1.4	Nanosphere: Fewer Homogeneous Nucleation and its Effect on Phase	
	Diagram	10
1.5	Nanosphere: Kirkendall Effect and Instability of Hollow Nanospheres	13
1.6	Nanosphere: Inverse Kirkendall Effect in Hollow Nano Alloy Spheres	17
1.7	Nanosphere: Combining Kirkendall Effect and Inverse Kirkendall Effect on	
	Concentric Bilayer Hollow Nanosphere	18
1.8	Nano Hole: Instability of a Donut-Type Nano Hole in a Membrane	19
1.9	Nanowire: Point Contact Reactions Between Metal and Silicon	
	Nanowires	21
1.10	Nanowire: Nanogap in Silicon Nanowires	22
1.11	Nanowire: Lithiation in Silicon Nanowires	26
1.12	Nanowire: Point Contact Reactions Between Metallic Nanowires	27
1.13	Nano Thin Film: Explosive Reaction in Periodic Multilayered Nano Thin	
	Films	28
1.14	Nano Microstructure in Bulk Samples: Nanotwins	30
1.15	Nano Microstructure on the Surface of a Bulk Sample: Surface	
	Mechanical Attrition Treatment (SMAT) of Steel	32
	References	33
	Problems	35

1.1 INTRODUCTION

In recent years, a new development in science and engineering is nanoscience and nanotechnology. It seems technology based on nanoscale devices is hopeful. Indeed, at the moment the research and development on nanoscale materials science for nanotechnology is ubiquitous. Much progress has been accomplished in the processing of

nanoscale materials, such as the growth of silicon nanowires. Yet, we have not reached the stage where the nanotechnology is mature and mass production of nanodevices is carried out. One of the difficulties to be overcome, for example, is the large-scale integration of nanowires. We can handle a few pieces of nanowires easily, but it is not at all trivial when we have to handle a million of them. It is a goal to be accomplished. For comparison, the degree of success of nanoelectronics from a bottom-up approach is far from that of microelectronics from a top-down approach. In reality, the bottom-up approach of building nanoelectronic devices from the molecular level all the way up to circuit integration is very challenging. Perhaps, it is likely that a hybrid device will have a better chance of success by building nanoelectronic devices on the existing platform of microelectronic technology and by taking advantage of what has been developed and what is available in the industry.

The proved success of microelectronic technology in the past and now leads to expectations of both high yield in processing and reliability in the applications of the devices. These requirements extend to nanotechnology. No doubt, reliability becomes a concern only when the nanodevices are in mass production. We may have no concern about their reliability at the moment because they are not yet in mass production, but we cannot ignore it if we are serious about the success of nanotechnology.

On processing and reliability of microelectronic devices, kinetics of atomic diffusion and phase transformations is essential. For example, on processing, the diffusion and the activation of substitutional dopants in silicon to form shallow p-n junction devices require a very tight control of the temperature and time of fabrication. It is worth mentioning that Bardeen has made a significant contribution to the theory of atomic diffusion on our understanding of the "correlation factor" in atomic jumps. On reliability, the issue of electromigration-induced failures is a major concern in microelectronics, and the kinetic process of electromigration is a cross-effect of irreversible processes. Today, we can predict the lifetime of a microelectronic device or its mean-time-to-failure by conducting accelerated tests and by performing statistical analysis of failure. However, it is the early failure of a device that concerns the microelectronic industry the most. Thus, we expect that in the processing and reliability of nanoelectronic devices, we will have similar concerns of failure, especially the early failure, which tends to happen when the integration processes and the reliability issues are not under control. It is for this reason that the kinetics of nanoscale materials is of interest. If we assume that everything in nanoscale materials and devices is new, it implies that the yield and reliability of nanodevices is new too, which we hope is not completely true. In this book, we attempt to bridge the link between a kinetic process in bulk and the same process in nanoscale materials. The similarity and the difference between them is emphasized, so that we can have a better reference of the kinetic issues in nanodevices and nanotechnology.

To recall kinetic processes in bulk materials, we note that there are several kinds of phase changes in bulk materials in which the distance of diffusion or the size of phases are in nanoscale. Take the case of Guinier–Preston (GP) zones of precipitation, in which the thickness of GP zone is of atomic scale and the spacing between zones is of the order of 10 nm. In the case of spinodal decomposition, the wave length of decomposition is of nanometers. In homogeneous nucleation, the distribution of subcritical nuclei is a distribution of nanosize embryos. In ripening, a distribution

of particles of nanoscale is assumed, and the analysis of ripening starts with the Gibbs-Thomson (GT) potential of these particles having a very small or nanoscale radius.

Furthermore, there are nanoscale microstructures in bulk-type materials. An example is the square network of screw dislocations in forming a small angle twist-type grain boundary. We can take two (001) Si wafer and bond them together face-to-face with a few degrees of misorientation of rotation, the dislocation network in the twist-type grain boundary forms one of the most regular two-dimensional nanoscale squares. Another example is a bulk piece of Cu that has a high density of nanotwins. One more example is a layer of nanosize grains formed by ball milling on the surface of a bulk piece of steel, which is called *surface mechanical attrition treatment (SMAT)* of nano-grains.

Our understanding of kinetic processes in bulk materials can serve as the stepping stone from where we enter into the kinetics in nanoregion. On seeing the similarity in kinetics between them, we can follow the similarity to reach a deeper level of understanding of the kinetic processes in nanoscale materials. On seeing the difference, we may appreciate what modification is needed in terms of driving force and/or kinetic process in nanoscale materials. In the early chapters of this book, several examples have been chosen for the purpose of illustrating the link between kinetic behaviors in bulk and in nanoscale materials, and in the later chapters a few cases of applications of nanoscale kinetics are given.

When we deal with nanoscale materials, we encounter very high gradient of concentration, very large curvature or very small radius, very large amount of nonequilibrium vacancies, very few dislocations, and yet very high density of surfaces and grain boundaries and, may be, nanotwins. They modify the driving force as well as the kinetic jump process. Indeed, the kinetic processes in nanoscale materials have some unique behavior that is not found in the kinetics of bulk materials. In this chapter of introduction, we present a few examples of nanoscale materials to illustrate their unique kinetic behavior. They are nanospheres, nanowires, nanothin films, and nanomicrostructures. More details will be covered in the subsequent chapters.

1.2 NANOSPHERE: SURFACE ENERGY IS EQUIVALENT TO GIBBS-THOMSON POTENTIAL

We consider a nanosize sphere of radius r. It has a surface area of $A = 4\pi r^2$ and surface energy of $E = 4\pi r^2 \gamma$, where γ is the surface energy per unit area and we assume that the magnitude of the surface energy per unit area γ is independent of r. We note that as surface energy is positive, the surface area (or the radius of the sphere) tends to shrink in order to reduce surface energy, which implies that the tendency to shrink exerts a compression or pressure to all the atoms inside the sphere. This pressure is called the *Laplace pressure*. The effect of the pressure is felt when we want to add atoms or remove atoms from the sphere because it will change the volume as well as the surface area. When we want to change the volume of the sphere under the Laplace pressure at constant temperature, we need to consider the work done and the work

equals to the energy change, so that $pdV = \gamma dA$. The pressure can be calculated as

$$p = \gamma \frac{dA}{dV} = \gamma \frac{(d/dr)(4\pi r^2)}{(d/dr)((4/3)\pi r^3)} = \gamma \frac{8\pi r}{4\pi r^2} = \frac{2\gamma}{r}$$
 (1.1)

However, we note that the work done by the Laplace pressure is different from the conventional elastic work done in a solid by a stress. The elastic work is given below,

$$E_{\rm elastic} = V \cdot \int \sigma d\varepsilon = V \frac{1}{2} K \varepsilon^2 \tag{1.2}$$

To calculate the elastic work, we need to know at least the elastic bulk modulus *K* of the material (in case of homogeneous hydrostatic stress). On the other hand, the work done by Laplace pressure is due to the change in volume by adding or removing atoms under the Laplace pressure, and no modulus is needed.

We consider the case of adding an atom to a nanosphere, the Gibbs free energy (G=U-TS+pV) increases $p\Omega$, where U is internal energy, T is temperature, S is entropy, and Ω is atomic volume. By definition, $p\Omega$ is a part of the chemical potential of the nanosphere related to the change of its volume under the fixed external pressure. It is the change (increase) of Gibbs free energy due to the addition of one atom (or one mole of atoms, depending on the definition of chemical potential) to the nanosphere (see Section 2.2.3, on the definition of chemical potential). It is worth mentioning that adding an atom at constant temperature has effects on U, S, and p. This is because it adds a few more interatomic bonds to U, the configuration entropy increases because of more ways in arranging the atoms, and though it does not affect the external pressure, the Laplace pressure will decrease because of the increase in radius.

Here it is important to distinguish two alternative approaches to account for surface (capillary) effects:

- 1. Helmholtz free energy F = U TS of the limited system includes explicitly an additional free energy of the surface: $F = N \cdot f + \gamma \cdot A$, where f is a bulk free energy per atom, N is the number of atoms, A is an area of external boundary (in our case $A = 4\pi R^2$), γ is an additional surface free energy per unit area. In this case the "p" in the expression for Gibbs energy is just real external pressure of the thermal ambient, without any Laplace terms. In this case, $G = F + pV = N \cdot (f + p\Omega) + \gamma \cdot A = Ng + \gamma \cdot A$. Then the chemical potential $\mu = \partial G/\partial N = g + \gamma \cdot (\partial A/\partial N)$. Below we start with this case.
- 2. Alternatively, free energy F = U TS of the limited system may not include explicitly the surface energy but instead use some effective external pressure $p^{\rm ef} = p + p_{\rm Laplace}$. Then $\mu = \mu^{\rm bulk} + p_{\rm Laplace} \cdot \Omega$. If $p_{\rm Laplace} = \gamma \cdot ((1/\Omega)(\partial A/\partial N))$, then the result will be the same.

To add the atom, if we imagine that the atomic volume Ω is "smeared" over the entire surface of the nanosphere as a very thin shell, it leads to the growth of the radius, dr, of the nanosphere as:

$$\Omega = dV = d\left(\frac{4}{3}\pi r^3\right) = 4\pi r^2 dr \Rightarrow dr = \frac{\Omega}{4\pi r^2}$$

so the work of Laplace pressure is $p_{\text{Laplace}}4\pi r^2 \times dr = p_{\text{Laplace}}\Omega = 2\gamma\Omega/r$, where the product of $p_{\text{Laplace}}4\pi r^2$ (force) and dr (distance) is the work done by the Laplace pressure. It is due to a surface change induced free energy change in the nanosphere, hence it should be added to the chemical potential of all the atoms belonging to the nanosphere. Thus, $p\Omega$ is the surface input into the chemical potential. We emphasize that this is an additional chemical potential energy of every atom in the nanosphere, not just the atoms on the surface, due to the surface effect. When r is small, this addition to chemical potential (GT potential), $2\gamma\Omega/r$, cannot be ignored.

Let us take the integral over the process of constructing the entire volume of the nanosphere by sequential adding of new spherical slices $4\pi r'^2 dr'$, and we obtain

$$\int_0^r p_{\text{Laplace}} dV = \int_0^r \frac{2\gamma}{r'} 4\pi r'^2 dr' = \gamma \cdot 4\pi r^2 = \Delta E_{\text{surface}}$$
 (1.3)

It means that the work done by Laplace pressure during the formation (growth) of the nanosphere is exactly equal to the surface energy. We have reached a very important conclusion that the surface energy $(4\pi r^2 \gamma)$ is equal to the sum of GT potential energy of all the atoms in the nanosphere, calculated as an integral over the evolution path of this sphere formation. (It is important to remember that in Eq. (1.3) the Laplace pressure under integral is not constant – it changes simultaneously with the growth of the sphere.) In other words, when we consider the GT potential, it means that all the atoms are the same, whether the atom is on the surface or within the nanosphere. We may say that from the point of view of GT potential, there is no surface atom, as all the atoms are the same, and hence there is no surface energy because the surface energy is being distributed to all the atoms.

To avoid possible misunderstanding, we emphasize that to form a nanosphere, we should add to the bulk energy an additional term of surface energy or the work of Laplace pressure, but not both of them. An example is in considering the formation energy of a nucleus in homogeneous nucleation, in which we include the surface energy of $4\pi r^2 \gamma$ explicitly, see Eq. (1.11) or Eq. (6.1), so we do not need to add GT potential to all the atoms, even though the radius of a nucleus is very small. Another example is in ripening, in which the kinetic process is controlled by the mean-field concentration in equilibrium with particles having the mean radius, following the GT equation, but the surface energy of $4\pi r^2 \gamma$ is implicit in the analysis, although the driving force comes from the reduction of surface energy. These two cases are covered in detail in later chapters.

As we can regard the hydrostatic pressure or Laplace pressure, p, as energy density or energy per unit volume, we might regard pV as the energy increase in a volume V under pressure. Strictly speaking, it is not completely correct. For example, the additional energy due to the existence of a surface is surface tension times the surface area: $\Delta E = \gamma 4\pi r^2$. However, the product $p_{\text{Laplace}}V$ is equal to $(2\gamma/r)(4/3)\pi r^3 = 2/3(\gamma \cdot 4\pi r^2)$. It is less by one-third from the surface energy of ΔE . As shown in Eq. (1.3), we need to take integration in order to obtain the correct energy.

We recall that when we consider the surface energy of a flat surface where the radius is infinite. In this case, the Laplace pressure is zero, so does the GT potential. Yet it does not mean the surface energy is zero. Instead, we use the number of broken

bonds to calculate the surface energy of a flat surface by considering the cleavage of a piece of solid into two pieces having flat surfaces. In the case of a nanosphere, we simply use $4\pi r^2 \gamma$ for its surface energy on the basis of GT potential. We recommend readers to analyze the above equations for the case when radius tends to infinity, spherical surface becomes more and more flat, Laplace pressure tends to zero, but total surface energy grows to infinity.

Next we might ask the question of a nonspherical particle, what is the chemical potential inside the nonspherical particle with curvature changing from one area of the surface to another area? In Appendix A, the concept of Laplace pressure is applied to nano-cubic particle and nano-disk particle, and the chemical potentials are given.

On the question of a hollow nanoparticle that has two surfaces, the inner and outer surfaces, the simple answer is that atoms at places with different curvatures possess different chemical potentials, and these potential differences or chemical potential gradient should enable surface and bulk diffusion to occur and lead to equalizing of curvatures. Nevertheless, the answer does not give a receipt of finding a spatial redistribution of chemical potential inside the particle if the temperature is low so that the smoothening proceeds only by surface diffusion. This gives us an example of the limit of applicability of thermodynamic concepts owing to slow kinetics: chemical potential is a self-consistent thermodynamic quantity assuming the condition of sufficiently fast diffusion kinetics. So, if diffusion is frozen at a low temperature, the driving force of chemical potential gradient has no response in such system or subsystem. We analyze the case of hollow nanospheres having two surfaces in a later section, assuming that atomic diffusion is fast enough for curvature change to happen.

1.3 NANOSPHERE: LOWER MELTING POINT

Nanosize will affect phase transition temperature besides pressure. Now we consider the melting of nanoparticles. Melting means transition from a crystalline phase to a liquid phase, where the crystalline phase is characterized by having a long range order (LRO). At the melting point, Gibbs free energy of the two phases is equal. The very notion of LRO for particles with the size of several interatomic distances or even several tens of nanometers becomes somewhat fuzzy, and the melting transition may become gradual within a temperature range, depending on the distribution of the nanoparticle size in the sample. Experimentally, we tend to measure the melting of a sample consisting of a large number of nanoparticles, rather than just one nanoparticle. Assuming that the melting temperature has an average value within a temperature range, we continue to define it as the temperature at which Gibbs free energy of the two phases is equal.

In Figure 1.1, a plot of Gibbs free energy versus the temperature of the liquid state and the solid state of a pure bulk phase having a flat interface is depicted by the two solid curves. We assume that the bulk sample has radius $r = \infty$. The two solid curves cross each other at the melting point of $T_{\rm m}$ $(r = \infty)$.

For solid nanoparticles of radius r, its Gibbs free energy curve is represented by one of the broken curves, and we note that the energy difference between the two curves of the solids is the GT potential energy of $p\Omega_s = 2\gamma_s\Omega_s/r_s$, where γ_s is the

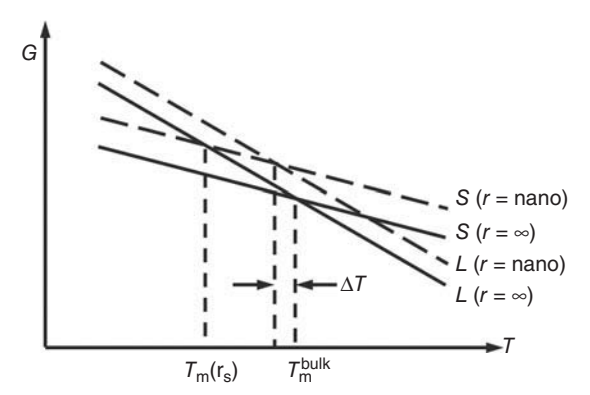


Figure 1.1 A plot of Gibbs free energy versus the temperature of the liquid state and solid state of a pure phase is depicted by the two solid curves. The two solid curves cross each other at the melting point of $T_{\rm m}$. We assume that the solid state of a bulk sample has radius $r=\infty$. For solid and liquid nanoparticles of radius $r_{\rm s}$ and $r_{\rm l}$, their Gibbs free energy curves are represented by the broken curves. The broken curves intersect at a lower temperature of $T_{\rm m}$ (nano), provided that we assume the surface energy of liquid is lower than that of the solid.

Interfacial energy between the solid and the ambient and it is independent of size. Usually we are interested in the melting point of nanoparticles in air or vacuum. Strictly speaking, if this ambient is infinite and if it does not contain the vapor of atoms of the same nanoparticle, and if we have unlimited time for observation, eventually these particles will evaporate totally. But we are not interested in this process; instead, we want to know what happens with the nanoparticles at a much shorter time (typically less than seconds), for example, if it is heated to some constant temperature below $T_{\rm m}$ ($r = \infty$), will it melt? In this case, the actual concentration of atoms in the vapor phase is unimportant unless it influences significantly the surface tension.

For liquid nanoparticles of radius r, its Gibbs free energy curve is represented by the other broken curve, and we note that the energy difference between the two curves of the liquid is the GT potential energy of $p\Omega_1 = 2\gamma_1\Omega_1/r_1$, where γ_1 is the interfacial energy between the liquid and the ambient.

The solid-state curve of nanoparticle typically (if $2\gamma_s\Omega_s/r_s > 2\gamma_l\Omega_l/r_l$) intersects the liquid state curve of $r=\infty$ at a lower temperature, $T_{\rm m}(r_{\rm s})$, indicating that the melting point of the nanoparticles (if many nanoparticles melt simultaneously forming bulk liquid with formally infinite radius of surface) is lower than that of the bulk solid having a flat surface. How much lower in the melting point will depend on γ and r for the solid state and the liquid state. Here is an analysis.

First, we can write the equilibrium condition at the melting point of the nanosolid and liquid particles as

$$\mu_{\rm s}^{\rm bulk} \left(T_{\rm m}^{\rm bulk} + \Delta T \right) + \frac{2 \gamma_{\rm s} \Omega_{\rm s}}{r_{\rm s}} = \mu_{\rm l}^{\rm bulk} \left(T_{\rm m}^{\rm bulk} + \Delta T \right) + \frac{2 \gamma_{\rm l} \Omega_{\rm l}}{r_{\rm l}}. \tag{1.4}$$

Expanding the chemical potentials into Taylor series over ΔT including only the first order terms (for not very big size effect) and taking into account that the derivative

of chemical potential over temperature is minus entropy, we obtain

$$\mu_{\rm s}^{\rm bulk} \left(T_{\rm m}^{\rm bulk} \right) - S_{\rm s} \Delta T + \frac{2\gamma_{\rm s} \Omega_{\rm s}}{r_{\rm s}} = \mu_{\rm l}^{\rm bulk} \left(T_{\rm m}^{\rm bulk} \right) - S_{\rm l} \Delta T + \frac{2\gamma_{\rm l} \Omega_{\rm l}}{r_{\rm l}}. \tag{1.5}$$

Then, taking into account the equality of the bulk chemical potentials for solid and liquid at the bulk melting temperature, the first term on both sides of the above equation cancels out. Using Clausius relation between the heat of transformation per atom $q_{\rm m}$ and entropy change per atom

$$\left[q_{\rm m} = \int_{\rm solid}^{\rm liquid} T dS = T_{\rm m}^{\rm bulk} \int_{\rm solid}^{\rm liquid} dS = T_{\rm m}^{\rm bulk} \cdot \left(S_{\rm l} - S_{\rm s}\right)\right],$$

we obtain:

$$\begin{split} S_{\mathrm{l}} - S_{\mathrm{s}} &= \frac{q_{\mathrm{m}}}{T_{\mathrm{m}}^{\mathrm{bulk}}} \\ &\frac{\Delta T}{T_{\mathrm{m}}^{\mathrm{bulk}}} = -\frac{\left(\left(2\gamma_{\mathrm{s}}\Omega_{\mathrm{s}}/r_{\mathrm{s}}\right) - (2\gamma_{\mathrm{l}}\Omega_{\mathrm{l}}/r_{\mathrm{l}})\right)}{q_{\mathrm{m}}} = -\frac{2\gamma_{\mathrm{s}}\Omega_{\mathrm{s}}}{q_{\mathrm{m}}r_{\mathrm{s}}} \left(1 - \frac{\gamma_{\mathrm{l}}}{\gamma_{\mathrm{s}}}\frac{\Omega_{\mathrm{l}}}{\Omega_{\mathrm{s}}}\frac{r_{\mathrm{s}}}{r_{\mathrm{l}}}\right) \end{split} \tag{1.6}$$

By taking into account the conservation of the number of atoms in the nanoparticle, $(4/3)\pi r_s^3/\Omega_s = (4/3)\pi r_l^3/\Omega_l$, we have finally:

$$\frac{\Delta T}{T_{\rm m}^{\rm bulk}} = -\frac{2\gamma_{\rm s}\Omega_{\rm s}}{q_{\rm m}r_{\rm s}} \left(1 - \frac{\gamma_{\rm l}}{\gamma_{\rm s}} \left(\frac{\Omega_{\rm l}}{\Omega_{\rm s}}\right)^{2/3}\right) \tag{1.7}$$

In Eq. (1.7), if we take $\gamma_1 = \gamma_s$ and $\Omega_1 = \Omega_s$, the bracket term becomes zero, it shows no temperature lowering. Typically, we can assume $\Omega_1 = \Omega_s$, and thus we have to assume too $\gamma_s > \gamma_1$, as depicted in Figure 1.1. Taking the following reasonable values for a metal,

$$\gamma_{\rm s} = 1.5 \,{\rm J/m^2}, \ \gamma_{\rm l} = 1 \,{\rm J/m^2}, \ \Omega_{\rm s} = \Omega_{\rm l} = 10^{-29} \,{\rm m^3}, \ q_{\rm m} = 2 \times 10^{-20} \,{\rm J}, \ r = 10^{-8} \,{\rm m}.$$

We obtain $\Delta T/T_{\rm m}^{\rm bulk} \approx -0.05$, so that the absolute value of melting temperature lowering, ΔT , is about 50° for a metal having a melting point about 1000 K.

It is worth mentioning that the lowering of the melting point due to small radius of solids has been studied long ago in the analysis of morphological instability of solidification in the growth of dendritic microstructures in bulk materials. It is a rather well developed subject by Mullins and Sekerka, so we discuss here only the key issue in solidification very briefly [1]. In Figure 1.2, a schematic diagram of the solidification front having a protrusion is depicted. The heat is being conducted away from the liquid side. Thus we can assume the bulk part of the solid has a uniform temperature of $T_{\rm m}$, but the liquid has a temperature gradient so the liquid in front of the solid is undercooled. The tip of the protrusion has a radius r. If we assume the radius is large and we can ignore the effect of GT potential on temperature, the temperature along

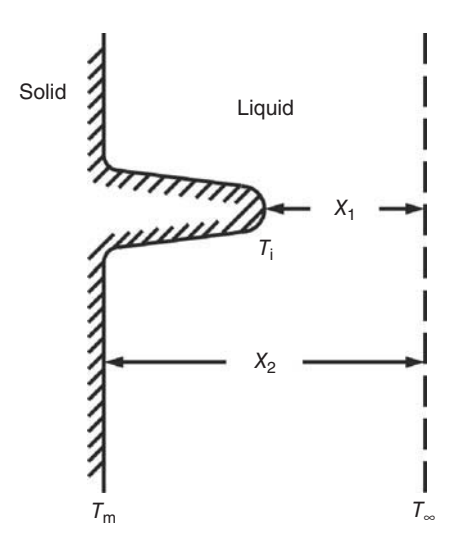


Figure 1.2 A schematic diagram of a solidification front having a protrusion.

the entire solid-liquid interface is $T_{\rm m}$ everywhere, including the tip. Now, in order to compare the temperature gradient in front of the tip and that in front of a point on the flat interface, we assume a uniform temperature T_{∞} in the liquid, which is less than $T_{\rm m}$, at a distance away from the front of solidification, as depicted in Figure 1.2. The temperature gradient in front of the tip of the protrusion is larger because $x_1 < x_2$.

$$\frac{T_{\rm m} - T_{\infty}}{x_1} > \frac{T_{\rm m} - T_{\infty}}{x_2} \tag{1.8}$$

The tip will advance into the undercooled liquid faster than the flat interface. Thus we have dendritic growth; in other words, the flat morphology of the growth front is unstable, and hence we have morphological instability.

However, if we assume now that the radius of the tip is of nanosize, we should consider the effect of GT potential on melting. In Figure 1.2, we assume that the melting point at the tip is $T_{\rm i}$, and $T_{\rm i} < T_{\rm m}$. With respect to T_{∞} , the temperature gradient in front of the tip has changed. For comparison, we have now

$$\frac{T_{\rm i} - T_{\rm \infty}}{x_1} \longleftrightarrow \frac{T_{\rm m} - T_{\rm \infty}}{x_2} \tag{1.9}$$

There is the uncertainty whether the gradient in front of the tip is larger or smaller than that in front of the flat surface. Because the radius of the tip tends to decrease with growth, the dentritic growth will persist. The optimal growth was found by solving the heat conduction equation and it occurs with the radius $r=2r^*$, where r^* is the critical radius of nucleation of the solid in the liquid at T_{∞} . In the growth of thermal dendrites, it is well known that besides primary arms, there are secondary and tertiary arms.

Low melting point of nanospheres may have an important application in microelectronic packaging technology: to lower the melting of Pb-free solder joints. In flip chip technology, solder joints of about $100\,\mu m$ in diameter are used to join Si chips to polymer-based substrate board. Owing to environmental concern, the microelectronic industry has replaced eutectic SnPb solder by the benign Pb-free solder. The latter, however, has a melting point about 220 °C, which is much higher than that of eutectic SnPb solder at 183 °C. The processing temperature or the so-called reflow temperature is about 30 °C above the melting point of the solder. The higher reflow temperature of Pb-free solder has demanded the use of dielectric polymer materials in the packaging substrate that should have a higher glass transition temperature. The use of polymer of higher glass transition temperature increases the cost of packaging. In addition, the higher reflow temperature also increases the thermal stress in the chip-packaging structure. Thus, solder paste of nanosize particles of Pb-free solder, the Sn-based solder, has been investigated for lowering the melting as well as the reflow temperature. Nevertheless, one of the complications that needs to be overcome is the fast oxidation of Sn nanoparticles in the solder paste.

1.4 NANOSPHERE: FEWER HOMOGENEOUS NUCLEATION AND ITS EFFECT ON PHASE DIAGRAM

Besides melting, other phase transformation properties of nanoscale particles can change with respect to bulk materials. We consider here the effect of nanoparticle size on homogeneous nucleation and then on phase diagrams. Generally speaking, in addition to pressure and temperature, GT potential will affect equilibrium solubility or composition, as shown by GT equation below

$$X_{\mathrm{B},r} = X_{\mathrm{B},\infty} \exp\left(\frac{2\gamma\Omega}{rkT}\right) \tag{1.10}$$

where $X_{B,r}$ and $X_{B,\infty}$ are the solubility of a solute at the surface of a particle of radius r and ∞ , respectively. As phase diagrams are diagrams of composition versus temperature, the equilibrium phase diagrams of bulk materials will be affected when it is applied to nanosize particles.

First, we consider the size effect on homogeneous nucleation in precipitation of an intermetallic compound phase, that is, nucleation within a nanoparticle of a supersaturated binary solid solution. We show that the homogeneous nucleation becomes very difficult and even suppressed.

In the precipitation of a supersaturated binary solid solution, we start from Figure 1.3, which is part of a bulk phase diagram of a two-phase mixture consisting of a practically stoichiometric compound "i," represented by the vertical line, and the boundary of the saturated solid solution, represented by the curved line 1, in Figure 1.3. When the solid solution is in the two-phase region, between the vertical line and the curved line, precipitation of the compound can occur by nucleation and growth.

The transformation starts from the formation of the critical nuclei of the compound phase in the supersaturated solution. For simplicity, we take the nuclei to be spherical. The change of the system's Gibbs free energy because of the nucleation of

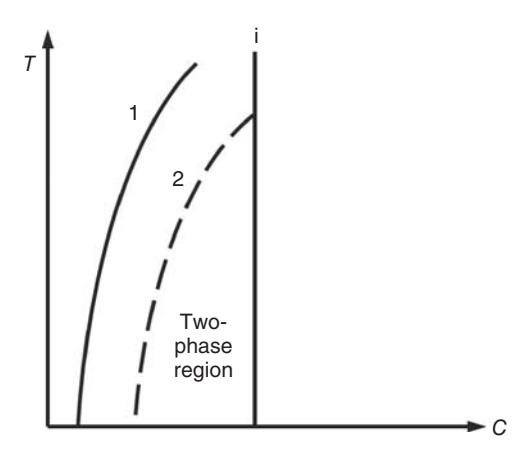


Figure 1.3 Part of a bulk phase diagram of a two-phase mixture consisting of a practically stoichiometric compound "i," the vertical line, and the saturated solid solution, the curved line 1. The broken curve represents the displacement of line 1 due to nanosize solid solution; it narrows down the two-phase region.

the compound sphere with radius r is

$$\Delta G(r) = -\Delta g \cdot \frac{(4/3) \cdot \pi r^3}{\Omega} + \gamma \cdot 4\pi r^2$$
 (1.11)

Here $((4/3) \cdot \pi r^3)/\Omega = n$ is the number of atoms in the spherical nucleus of radius r, Ω is atomic volume, Δg is a bulk driving force per one atom of the nucleus (the gain in energy per atom in the transformation), and γ is surface energy per unit area of the nucleus. The driving force, Δg , for macroscopic samples, can be calculated from the construction shown in Figure 1.4 and it is equal to

$$\Delta g = g_{\alpha}(\overline{C}) + (C_i - \overline{C}) \frac{\partial g_{\alpha}}{\partial C} \Big|_{\overline{C}} - g_i$$
 (1.12)

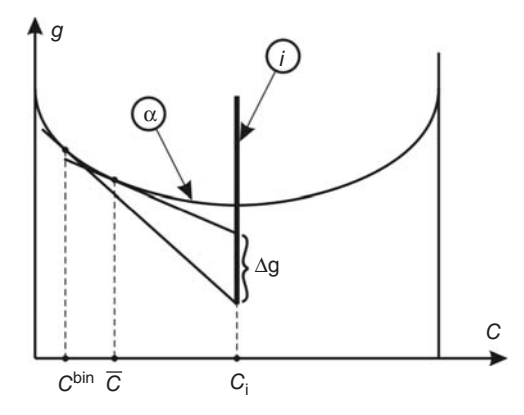


Figure 1.4 The driving force, Δg , for macroscopic samples, can be calculated from the tangent construction as shown. Qualitative concentration dependence of the Gibbs free energy per atom of parent phase α and of line compound phase i with $C_i = 1/2$. Composition C^{bin} of the bulk parent phase in the equilibrium with intermediate phase is determined by the common tangent. The driving force Δg of the bulk transformation is determined by the supersaturation magnitude.

Dependence of $\Delta G(r)$ on r has a maximum (nucleation barrier) at the critical size, at which the first derivative $d\Delta G(r)/dr$ is equal to zero. We obtain

$$r_{\rm cr} = \frac{2\gamma\Omega}{\Delta g} \tag{1.13}$$

and the height of the nucleation barrier is

$$\Delta G^* = \Delta G(r_{\rm cr}) = -\Delta g \cdot \frac{(4/3) \cdot \pi r_{\rm cr}^3}{\Omega} + \gamma \cdot 4\pi r_{\rm cr}^2 = \frac{1}{3} \gamma \cdot 4\pi r_{\rm cr}^2$$
 (1.14)

The formation of the critical nucleus of the compound with a fixed composition, c_i , needs the fixed number of the solute atoms or B atoms as given below.

$$N_{\rm B}^{\rm cr} = C_{\rm i} \cdot n_{\rm cr} = C_{\rm i} \cdot \frac{4\pi r_{\rm cr}^3}{3\Omega} = C_{\rm i} \cdot \frac{4\pi}{3\Omega} \cdot \left(\frac{2\gamma\Omega}{\Delta g}\right)^3 \tag{1.15}$$

where $n_{\rm cr}$ is the total number of atoms in the critical nucleus. If the precipitation proceeds within a limited volume (nanoparticle), we clearly need to consider the limitation due to the fact that a nanoparticle has a finite total number of B atoms;

$$N_{\rm B}^{\rm tot} = \overline{C} \cdot N = \overline{C} \frac{(4/3) \cdot \pi R^3}{\Omega}$$

where \overline{C} is the fraction of B atoms in the nanoparticle, and R is the radius of the nanoparticle, and N is the total number of atoms in the nanoparticle of radius R. Thus, nucleation (and the transformation as a whole) becomes impossible if

$$C_{\rm i} \cdot \frac{4\pi r_{\rm cr}^3}{3\Omega} > \overline{C} \cdot \frac{4\pi R^3}{3\Omega} \Longleftrightarrow R < \left(\frac{C_i}{\overline{C}}\right)^{1/3} r_{\rm cr}$$
 (1.16)

For example, if $r_{\rm cr}=1\,{\rm nm},~C_{\rm i}=1/2,~\overline{C}=0.02$, then nanoparticle of sufficiently small size, $R<\approx 3\,{\rm nm}$, cannot have homogeneous nucleation as considered above. Moreover, we expect that even for larger sizes, when nucleation is theoretically possible, the barrier will be high, making the probability of transformation practically impossible. In order to make nucleation possible, we need to increase the concentration of B atoms in the nanoparticle, in turn, we have to move the phase boundary of nanoparticles to a much higher concentration. Combining with a lower melting point of the nano compound phase, we show in Figure 1.3 the phase boundary of nanoparticles by the broken curve, line 2. The two-phase region for nanoparticles is actually narrower than that of the bulk phase.

The above consideration is based on homogeneous nucleation; however, we have to consider heterogeneous nucleation in nanoparticles. Nevertheless, it is known that the crystallization temperature in small droplets of high purity water can be lowered because of the suppression of heterogeneous nucleation as well as the difficulty of homogeneous nucleation. If we assume a high-purity nanoparticle and also assume that the surface energy of the compound phase is higher than that of the nano solid solution phase, the heterogeneous nucleation can be ignored.

1.5 NANOSPHERE: KIRKENDALL EFFECT AND INSTABILITY OF HOLLOW NANOSPHERES

Hollow nanoparticles of CoO or $\mathrm{Co_3S_4}$ were formed when Co nanoparticles were annealed in oxygen or sulfur atmosphere, respectively [2]. The formation of the hollow nanoparticles was explained on the basis of Kirkendall effect by assuming that the out-diffusion of Co is faster than the in-diffusion of oxygen or sulfur during the annealing. We recall that the Kirkendall effect was originally observed in bulk diffusion couple of Cu and CuZn [3]. Markers of Mo wire were placed at the original interface between the Cu and the CuZn. After interdiffusion, the markers were found to have moved into CuZn, indicating that the Zn atomic flux ($J_{\rm A}$) is greater than that of Cu atomic flux ($J_{\rm B}$). The unbalance of the two atomic fluxes in the interdiffusion has to be balanced by a flux of vacancies,

$$J_{\rm V} = J_{\rm A} - J_{\rm B}$$

which is directed toward the faster diffusing component. (Here we took the absolute values of the fluxes, to show explicitly that the vacancy flux is the difference of two atomic fluxes by absolute value.) Thus, to have void formation within a nanoparticle, we should place the faster diffusing component inside.

The flux of vacancy may or may not lead to void formation. When the vacancy concentration is assumed to be equilibrium everywhere in the bulk diffusion couple, no void forms. Indeed, in Darken's analysis of interdiffusion, there is no void formation because he has assumed that vacancy is in equilibrium everywhere in the diffusion couple. This is because the nucleation of a void requires the supersaturation of vacancy "vapor" or, in other words, the nonequilibrium vacancies.

In a nanosphere, the confinement of vacancies within the spherical shell structure will enable vacancies to accumulate and reach the supersaturation needed to nucleate a void. However, when we consider interdiffusion in a nanosphere, besides Kirkendall effect, we need to consider inverse Kirkendall effect, which is discussed in Section 1.5. Now we consider the role of curvature or the GT effect on the stability of a hollow nanosphere.

Figure 1.5a is a schematic diagram of the cross-section of a hollow nanosphere of a pure phase, in which r_1 and r_2 are the inner and outer radius, respectively. If we consider GT potential of both surfaces, an atom as well as a vacancy in the hollow sphere will be driven to diffuse by the potential gradient between the two surfaces. Here we take three approaches to consider the instability issue.

First, the inner surface has a negative curvature, but the outer surface has a positive curvature. The chemical potential of atoms near r_1 and r_2 are

$$\mu_1\left(=\mu_0+\frac{2\gamma}{-r_1}\Omega\right)<\mu_2\left(=\mu_0+\frac{2\gamma}{r_2}\Omega\right) \tag{1.17}$$

where μ_0 refers to the chemical potential of atoms in bulk materials. Under the potential gradient, atoms will diffuse from the outer surface to the inner surface, and the vacancies will diffuse in the opposite direction, leading to the elimination of the void

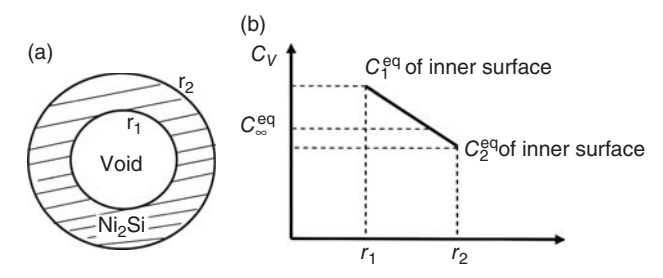


Figure 1.5 (a) A schematic diagram of the cross-section of a hollow nanosphere, in which r_1 and r_2 are the inner and outer radius, respectively. (b) A schematic diagram depicts the vacancy gradient across the shell of the hollow nanosphere.

and to transform the hollow nanosphere to a compact nanosphere finally. Figure 1.5b depicts the vacancy gradient across the shell of the hollow nanosphere. While vacancy concentration gradient inside the shell must be hyperbolic, to be shown later, we approximate it by a straight line because the distance is very short.

The second way is to look at the vacancy gradient by considering the radial stress potential difference between the inner and the outer surface. Because surface energy is positive, both surfaces tend to shrink. The tendency of shrinking of the inner surface exerts a radial tensile stress in the region near the inner surface. Following the Nabarro–Herring model of stress potential in analyzing creep, under tension, it is easier to form vacancies in the tensile region because the formation of a vacancy requires breaking bonds and it is easier to break those bonds that are already stretched under tension. Thus there are more vacancies near the inner surface with respect to the equilibrium vacancy concentration in a region without hydrostatic pressure or stress. In comparison, the outer surface exerts a radial compressive stress to atoms nearby, so there are fewer vacancies. Thus, the vacancy concentration gradient as shown in Figure 1.5b will lead to the diffusion of vacancies from the inner surface to the outer surface.

To avoid misunderstanding, one should remember that even in case of tensile stresses at inner surface and compressive stresses at external surface, the gradient of hydrostatic stress (one-third of the trace of stress tensor) inside spherical or cylindrical layer is zero. (Radial component changes, two tangential components change, and their sum is the same in each point inside shell.) There is no hydrostatic stress gradient inside shell; there is just difference of vacancy concentrations at the boundaries: vacancies diffuse from the inner boundary to the external one not because of some mechanical force, but due to entropic reasons – they diffuse from place with higher concentration (in the vicinity of inner boundary) to the place with lower concentration (in the vicinity of external boundary).

The third way is to examine the work done to form a vacancy in the inner as well as the outer surfaces. In this case, we first consider the formation of a vacancy near the inner surface. We remove an atom near the inner surface in order to leave a vacancy there, and we place the atom on the inner surface, meaning a shrinking of the inner surface (decrease of surface energy). Indeed, if we imagine that the atom of volume Ω is taken from the "bulk" and is "smeared" over the inner spherical surface of radius

 r_1 , then this radius should be reduced by $dr_1 = -\Omega/4\pi r_1^2$. The corresponding change of surface energy or work done for the formation of such a vacancy is $d(\gamma \cdot 4\pi r_1^2) = \gamma 8\pi r_1 dr_1 = \gamma 8\pi r_1 \cdot (-\Omega/4\pi r_1^2) = -2\gamma \Omega/r_1$. Similarly, we can obtain the change of surface energy or work done due to the formation of a vacancy near the outer surface, and it is positive and equal to $2\gamma \Omega/r_2$. It means that it is easier to form a vacancy near the inner surface than that in the outer surface. The equilibrium vacancy concentration near the inner and the outer surfaces are, respectively,

$$\begin{split} C_{\mathrm{V}}^{\mathrm{eq}}(r_1) &= \exp\left(-\frac{\left(E_{\mathrm{V}}^{\infty} - \left(2\gamma\Omega/r_1\right)\right)}{kT}\right) = C_{\mathrm{V}}^{\mathrm{eq}} \exp\left(\frac{2\gamma\Omega}{kTr_1}\right) \text{ and } \\ C_{\mathrm{V}}^{\mathrm{eq}}(r_2) &= \exp\left(-\frac{\left(E_{\mathrm{V}}^{\infty} + \left(2\gamma\Omega/r_2\right)\right)}{kT}\right) = C_{\mathrm{V}}^{\mathrm{eq}} \exp\left(-\frac{2\gamma\Omega}{kTr_2}\right) \end{split} \tag{1.18}$$

where $C_{\rm V}^{\rm eq}$ is the equilibrium vacancy concentration in the bulk. Thus, the vacancy concentration gradient as shown in Figure 1.5b, will lead to the diffusion of vacancies from the inner surface to the outer surface.

The overall result is in agreement with an energy consideration based on the total surface area. By conservation of volume, we have for the transformation of a hollow sphere to a solid sphere,

$$\frac{4}{3}\pi r_2^3 - \frac{4}{3}\pi r_1^3 = \frac{4}{3}\pi r_0^3$$

where r_0 is the radius of the solid sphere. The reduction in surface area will be

$$4\pi r_0^2 < 4\pi (r_2^2 + r_1^2)$$

In the hollow shell structure as shown in Figure 1.5a, we cannot define what is the equilibrium concentration of vacancies. As there are two surfaces with different potential to serve as references for source and sink of vacancies, no equilibrium vacancy concentration can be given. System will reach equilibrium vacancy concentration only after reaching equilibrium shape, which is after the collapse of a hollow shell into a compact particle. This is unique in a hollow nanosphere. If we assign a vacancy concentration corresponding to the equilibrium vacancy concentration with respect to a planar surface in a bulk sample, $C_{\rm V}^{\rm eq}$, it is between the vacancy concentration at r_1 and r_2 .

If we anneal the hollow nanosphere at a high temperature to enhance diffusion, the void at the core of the nanosphere will disappear. To estimate the time scale for the filling of a hollow nanosphere, a single elemental phase is assumed for simplicity. If the inner and outer radii of the shell are not too small $(r_i \gg (2\gamma\Omega/kT) \equiv \beta)$, then the exponents in the above equations can be expanded, so that we can take the vacancy

concentration near the inner surface, r_1 , and the outer surface, r_2 , respectively, to be

$$C_{v}(r_{1}) = C_{v}^{eq} \left(1 + \frac{\beta}{r_{1}} \right)$$

$$C_{v}(r_{2}) = C_{v}^{eq} \left(1 - \frac{\beta}{r_{2}} \right)$$

$$(1.19)$$

where $\beta = 2\gamma \Omega/kT$, and γ is the surface energy per unit area, Ω is atomic volume, and kT has the usual meaning. We show here that we can use the vacancy concentrations in Eq. (1.19) as the boundary conditions for the diffusion equation in the nanosphere.

In spherical coordinates and if we assume a steady state process, the diffusion equation can be expressed as

$$\nabla^2 C = \frac{\partial^2 C}{\partial r^2} + \frac{2}{r} \frac{\partial C}{\partial r} = \frac{1}{r^2} \frac{\partial}{\partial r} \left(r^2 \frac{\partial C}{\partial r} \right) = 0 \tag{1.20}$$

which means

$$r^2 \frac{\partial C}{\partial r} = \text{const} = -B, \quad dC = -B \frac{dr}{r^2}$$

By integration, we obtain the solution of the diffusion equation to be C(r) = B/r + A. By using Eq. (1.19) as boundary conditions, we have

$$\begin{split} C_{\mathrm{v}}(r_1) &= \frac{B}{r_1} + A = C_{\mathrm{v}}^{\mathrm{eq}} \left(1 + \frac{\beta}{r_1} \right) \\ C_{\mathrm{v}}(r_2) &= \frac{B}{r_2} + A = C_{\mathrm{v}}^{\mathrm{eq}} \left(1 - \frac{\beta}{r_2} \right) \end{split}$$

By solving the last two equations for A and B, we have

$$\begin{split} B &= C_{\mathrm{v}}^{\mathrm{eq}} \beta \frac{r_2 + r_1}{r_2 - r_1} \\ A &= C_{\mathrm{v}}^{\mathrm{eq}} \left(1 - \frac{2\beta}{r_2 - r_1} \right) \end{split}$$

So we obtain the concentration profile of vacancies as [4],

$$C_{v}(r) = C_{v}^{eq} \beta \left(\frac{r_{2} + r_{1}}{r_{2} - r_{1}}\right) \frac{1}{r} + C_{v}^{eq} \beta \left(-\frac{2}{r_{2} - r_{1}}\right) + C_{v}^{eq}$$
(1.21)

Knowing $C_v(r)$, we can calculate its first derivative at r_1 . Then, using Fick's first law of diffusion, we obtain the total flux of vacancies, J, leaving (or atoms arriving at) at the spherical surface of r_1 . The volume of the void is $V = (4/3)\pi(r_1)^3$, the number of atoms needed to fill the void is $N = V/\Omega$, where Ω is the atomic volume. We can take N = JA't, where A' the surface area of the void and t is time, but A' is shrinking with time; instead, we can take N = Jt, where T is an average total flux during shrinking

and t is the shrinkage time, and the time needed to fill the void can be estimated roughly to be

 $t \cong \frac{kT}{A\gamma D\Omega} r_1^3 \tag{1.22}$

where A is a constant of the order of 10, and $D \approx D_{\rm v} C_{\rm v}^{\rm eq}$ is the self-diffusion coefficient of the atoms in the nanosphere.

If we take Au as an example because we know its surface energy and self-diffusivity very well, $\gamma = 1400\,\mathrm{erg/cm^2}$ and $D = 0.1 \times \mathrm{exp} - (1.8\,\mathrm{eV})/\mathrm{kT}\,\mathrm{cm^2/s}$. Assume a hollow nanosphere having $r_1 = 30\,\mathrm{nm}$ and $r_2 = 60\,\mathrm{nm}$, it will take about $5 \times 10^3\,\mathrm{s}$ at $400\,^{\circ}\mathrm{C}$ to transform the hollow nanosphere to a solid nanosphere. In the case where the hollow particles has $r_1 = 3\,\mathrm{nm}$ and $r_2 = 6\,\mathrm{nm}$, the required transformation time is only a few seconds.

We can simplify the above analysis, without solving the diffusion equation in spherical coordinates, by assuming that the vacancy flux is steady because the thickness of the nanoshell is extremely small, and thus the vacancy flux is given as

$$J_{V} = -D_{V} \frac{\Delta C_{V}}{\Delta r} = -D_{V} C_{V}^{eq} \frac{(1 + (\beta/r_{1})) - (1 - (\beta/r_{2}))}{r_{1} - r_{2}}$$

$$= -D_{V} C_{V}^{eq} \beta \frac{((1/r_{1}) + (1/r_{2}))}{r_{1} - r_{2}}$$

$$= D_{V} C_{V}^{eq} \frac{2\gamma \Omega}{kT} \left(\frac{1}{r_{1}} + \frac{1}{r_{2}}\right) \frac{1}{\Delta r}$$
(1.23)

where $\beta=2\gamma\Omega/kT$ and $\Delta r=r_2-r_1$. Then we assume this average vacancy flux will remove the void in time "t" and we take $(4/3)(\pi r_1^3)(1/\Omega)=J_{\rm V}(4\pi r_1^2)t$. We reach the same conclusion as that given by Eq. (1.22).

We can have several kinds of nano hollow spheres; they are a pure element, an intermetallic compound phase, an alloy phase, and a coaxial bilayer structure. We have discussed here the kinetic behavior of nano hollow spheres of a pure element. In the following section, we consider nano hollow spheres of an alloy or solid solution phase for the consideration of inverse Kirkendall effect. Then we study the nano hollow spheres having a coaxial bilayer structure for the consideration of interdiffusion. More detailed studies are presented in Chapter 3.

1.6 NANOSPHERE: INVERSE KIRKENDALL EFFECT IN HOLLOW NANO ALLOY SPHERES

If the hollow nanosphere is an alloy phase, the vacancy diffusion as discussed in the previous section will induce the inverse Kirkendall effect. The classic Kirkendall effect of interdiffusion in a diffusion couple of A and B showed that when the flux of A is not equal (by absolute value) to the counter flux of B, a vacancy flux will be generated to balance the interdiffusion. The inverse Kirkendall effect refers to the effect when a preexisting vacancy flux (generated by some external force) affects the

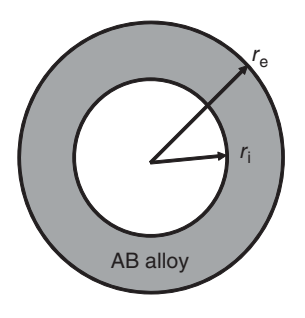


Figure 1.6 A schematic diagram depicts a homogeneous AB alloy with a hollow shell structure. A vacancy gradient exists and the vacancy diffusion from the inner side to the outer side, and consequently, will lead to dealloying when the intrinsic diffusion of A and B is different.

interdiffusion of A and B in a homogeneous alloy of AB. A classic example is the irradiation of a homogeneous alloy in a nuclear reactor. Under irradiation, segregation in a homogeneous AB alloy occurs and the alloy becomes inhomogeneous because the irradiation has produced excess vacancies and in turn a flux of vacancy in the alloy. The diffusion of the vacancies has led to the interdiffusion and segregation of A and B in the homogeneous alloy.

We consider a homogeneous AB alloy with a hollow shell structure, as shown in Figure 1.6. When such a hollow nanoshell is annealed at a constant temperature, dealloying or segregation of A and B occurs. This is different from thermomigration or the Soret effect, which occurs when a homogeneous alloy is annealed in a temperature gradient. The segregation in the nano shell alloy takes place isothermally, so there is no temperature gradient. Following GT effect, there will be a higher vacancy concentration near the inner shell surface than that near the outer shell surface. Because of the vacancy concentration gradient, a vacancy flux exists, and the diffusion of vacancies will affect the diffusion of A and B atoms. If we assume that the intrinsic diffusivity of A and B are different, it leads to dealloying or segregation in the hollow alloy shell. The faster diffusing species will segregate to the inner shell and create a gradient of chemical potential to retard the vacancy flux. The diffusion of A and B is uphill. Provided that the vacancy potential is larger than the counterpotential of dealloying, the hollow alloy shell will eventually transform to a solid nanosphere in order to reduce the total surface area, but the rate is typically slower than that of a pure phase. The kinetic analysis is presented in Chapter 3.

1.7 NANOSPHERE: COMBINING KIRKENDALL EFFECT AND INVERSE KIRKENDALL EFFECT ON CONCENTRIC BILAYER HOLLOW NANOSPHERE

When we consider the interdiffusion of A and B in a planar two-layer structure as shown in Figure 1.7a, we have only the Kirkendall effect when the atomic fluxes of A and B are unequal. When we bend the planar bilayer into a nano shell having a coaxial bilayer structure, as shown in Figure 1.7b, the Kirkendall effect and inverse Kirkendall effect coexist [5]. How they interact with each other is not straightforward and it requires a careful analysis.

If A is the outer layer and B is the inner layer and if the flux of A, J_A , is bigger than the flux of B, J_B , the balancing vacancy flux, J_V , due to Kirkendall effect, will